Technical Report No. 9

ESTIMATION OF LAND SURFACE TEMPERATURE USING AVHRR SENSORS ON THE NOAA SATELLITE

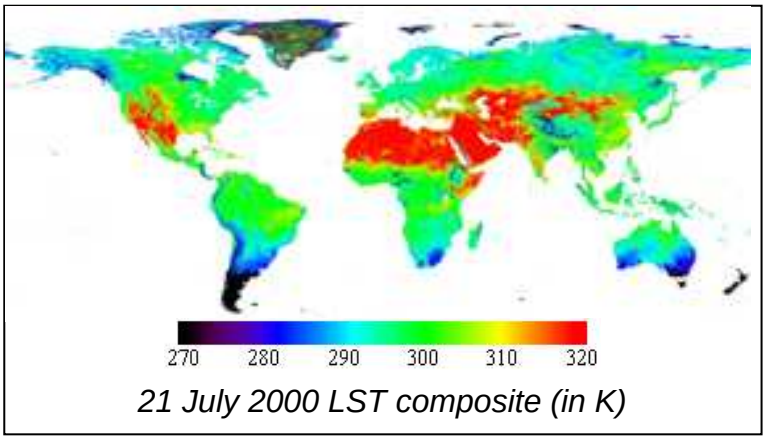

21 July 2000 LST composite (in K)

Author names: J. A. Sobrino, Y. Julien, V. Hidalgo, J.C. Jimenez, G. Soria, C. Mattar, B. Franch, R. Oltra, J. Cuenca.

Date: 10 December 2008.

WATCH is an Integrated Project Funded by the European Commission under the Sixth Framework Programme, Global Change and Ecosystems Thematic Priority Area (contract number: 036946).
The WACH project started 01/02/2007 and will continue for 4 years.

Title:	LST ESTIMATION FROM NOAA-AVHRR DATA
Authors:	J. A. Sobrino, Y. Julien, V. Hidalgo, J.C. Jimenez, G. Soria, C. Mattar, B. Franch, R. Oltra, J. Cuenca.
Organisations:	University of Valencia, Spain
Submission date:	10 December 2008
Function:	This report is an output from Work Block 1; task 1.1
Deliverable	WATCH deliverable 1.1.2

ABSTRACT

The theoretical basis for the land surface temperature (LST) and land surface emissivity (LSE) retrieval from the Advanced Very High Resolution Radiometer (AVHRR) is given, using split-window techniques.

The algorithms proposed use calibrated reflectances and brightness temperatures from the AVHRR channels 1, 2, 4, 5 as well as NDVI images to produce a global LST.
The algorithms can be used globally as they have been simulated from a worldwide emissivity and brightness temperature data base.
The cloud tests applied to the LST data are also provided.

This document describes the mathematical basis for the algorithms, the ancillary data-sets required and the validation strategy.

TABLE OF CONTENTS

1.- INTRODUCTION

This Algorithm Theoretical Basis Document (ATBD) describes a set of algorithms that make use of the split-window (SW) techniques to retrieve land surface temperature (LST) from Level 1B data generated by the Advanced Very High Resolution Radiometer (AVHRR) of the American National Oceanic and Atmospheric Administration (NOAA).

This document identifies the sources of input data, outlines the physical principles and mathematical background, described the proposed algorithms and lists the assumptions and limitations of this technique.

2.- BACKGROUND

2.1- Scientific Objectives and Justification

The measurement of Land Surface Temperature (LST) from thermal infrared images is of considerable importance for many applications such as oceanography, global climate studies, geology, hydrology, meteorology and vegetation monitoring. Most of the fluxes at the surface-atmosphere interface can only be parameterized through the use of LST. In comparison with sea surface, land surface has the additional difficulty of the high heterogeneity, mainly due to vegetation, topography and soil physical properties and the complex relationship between atmosphere and surface.

Conventional temperature measurements are very isolated in time and space, and are therefore very difficult to extend to larger scales, mainly because of the heterogeneity of the surface. The use of satellite images instead of in situ values could be possible if the measurement techniques give LST value with sufficient accuracy. The satellite-measured radiance must be corrected due to atmospheric perturbation and an emissivity value different from unity because natural surfaces are not blackbodies.

2.2.- Previous Approaches

Several theoretical studies developed LST algorithms through split-window (SW) (Price, 1984; Becker and Li, 1990a; Sobrino et al., 1991; Prata, 1993; Sobrino et al., 1994, etc) methods applicable to different sensors, as AVHRR, Thematic Mapper, MODIS, ASTER and AATSR series of instruments.

The SW method uses observations at two different spectral bands within 10-12 μm spectral region to eliminate the influence of the atmosphere. The benefit of the SW method is based upon the fact that the atmospheric absorption of the surface radiation varies strongly with wavelength, and so, atmospheric effects can be corrected by using data from two different spectral channels. Since the water vapor continuum absorption coefficients in the thermal infrared band are not well known, the coefficients from the split-window algorithm depend strongly on the transmission code used (Grant 1990).

2.3.- Instrument Characteristics

The NOAA satellite series, NOAA-7, -9, -11, -14 and -16 follow polar, sun synchronous orbits with nadir afternoon overpass times. NOAA-7 data span the years 1981-1985, NOAA-9, 1986-1989, NOAA-11, 1989-1995, NOAA-14, 1995-2000, and NOAA-16 (see figure 1) from 2000 to 2004 (and continues through the present). Data from NOAA-9 was used from September 1994 until January 1995 when NOAA-11 started to malfunction and its replacement, NOAA-13, failed shortly after launch.

The AVHRR is a scanning, imaging radiometer, scanning ± 55 degrees, providing a 2800 km swath width. This swath width is greater than the 25.3 degrees separation between successive orbital tracks and provides overlapping coverage (side-lap). The orbital configuration permits daily coverage at a maximum spatial resolution (in nadir direction) of 1 km of each point on earth, although at different viewing and illumination geometries on subsequent days. The orbital period of about 102 minutes produces 14.1 orbits per day. Because the daily number of orbits is not an integer, the suborbital tracks do not repeat daily, although the local solar time of the satellite's passage is essentially unchanged for any latitude. The orbit repeats its ground track each 9 days.

Three different models of the AVHRR instrument can be distinguished: AVHRR/1, AVHRR/2 and AVHRR/3. The latter is the one on board the KLM (NOAA-15, -16...) series satellites. The AVHRR instrument provides with data from different portions of the visible (0.6 μm), near infrared (0.9 μm) and thermal infrared (3.7, 11 and 12 μm) spectrum. Observation from channels corresponding to the visible and near infrared allows the study of vegetation, clouds, lakes, coasts, snow and ice. The three remaining channels operating in the thermal infrared allow obtaining products for land, water, and sea surface and clouds temperature. The additional 3A channel (1.6 μm) present in AVHRR/3 improves the capability for distinguishing among snow, ice and clouds.

Figure 1: NOAA-16.

There is now a massive archive of images from the AVHRR that can be used to produce global and regional maps of LST for a 20-year period beginning in 1981, compiled in the Pathfinder AVHRR Land (PAL) database.

3.- ALGORITHM

3.1- Overview

The structure of the theoretical algorithms was obtained from the radiative transfer equation, considering the at-sensor radiance ($L_{\lambda}^{at-sensor}$) for a given wavelength (λ) as:

$$L_{\lambda\theta}^{at-sensor} = \left[\varepsilon_{\lambda\theta} B_{\theta}(\lambda, T_S) + (1-\varepsilon_{\lambda\theta}) L_{\lambda}^{atm\downarrow}\right] \tau_{\lambda\theta} + L_{\lambda\theta}^{atm\uparrow} \quad (1)$$

where $\varepsilon_{\lambda\theta}$ is the surface emissivity, $B_\theta(\lambda, T_s)$ is the radiance emitted by a blackbody (BB) at temperature T_s of the surface, $L_{\lambda}^{atm\downarrow}$ is the downwelling radiance, $\tau_{\lambda\theta}$ is the total transmission of the atmosphere (transmittance) and $L_{\lambda\theta}^{atm\uparrow}$ is the upwelling atmospheric radiance. All these magnitudes also depend on the observation angle θ.

The expression for B (λ, T_s) is given by the Planck's law:

$$B(\lambda, T_S) = \frac{c_{1L}\lambda^{-5}}{\exp\left(\frac{c_2}{\lambda T_S}\right) - 1} \quad (2)$$

with c_{1L} = 1.19104·10^8 W μm^4 m^{-2} sr^{-1} and c_2 = 1.43877·10^4 μm K, the first radiation constant (for spectral radiance) and second radiation constant, respectively, B (λ, T_s) is given in W m^{-2} sr^{-1} μm^{-1} if λ is given in μm.

According to Sobrino et al. (1996), the upwelling and downwelling atmospheric radiance can be substituted, respectively, by:

$$L_{\lambda}^{atm\uparrow} = (1-\tau_{i\theta})\, B_i(T_a) \quad (3)$$

$$L_{\lambda}^{atm\downarrow} = (1-\tau_{i53}) B_i(T_a) \quad (4)$$

where T_a is the effective mean atmospheric temperature and τ_{i53} is the total atmospheric path transmittance at 53 degrees.

Substituting both atmospheric radiances (3) and (4) in the radiative transfer equation (1), an algorithm involving temperatures can be obtained using a first-order Taylor series expansion of the Planck's law and writing the equation for i and j (i and j being two different channels observed at the same angle, SW method):

$$T_s = T_i + A(T_i - T_j) - B_0 + (1-\varepsilon_i) B_1 - \Delta\varepsilon_\theta\, B_2 \quad (5)$$

where A and B_i are coefficients that depend on atmospheric transmittances, ε_i is the mean value of the emissivities of channels i and j, $\Delta\varepsilon_\theta$ is the spectral variation of the emissivity, T_i and T_j are the brightness temperatures for two different channels with the same view angle. Using equation (5) we can get a separation between the atmospheric and emissivity effects in the retrieval of surface temperature.

3.2.- Processing

To give operational algorithms, apart from the surface emissivity, atmospheric temperature and transmissivity must be known in the area studied and for each atmospheric situation. The determination of the split-window coefficients has been made using simulations because there is no sufficient volume of high quality *in situ* measurement of LST coincident with AVHRR temperatures, to permit a good determination of the coefficients. Therefore, the necessary data for the regression have been obtained from radiative transfer simulations, as has been done at NOAA for SST determination (McClain et al., 1985), and subsequently the algorithms obtained have to be validated with *in situ* measured data.

MODTRAN radiative transfer code (Abreu and Anderson, 1996) is used to calculate the brightness temperatures expected at the satellite for 61 different situations. The vertical profiles of temperature and water vapor content for these situations were obtained from the radiosoundings extracted carefully from the TOVS (TIROS Operational Vertical Sounder) initial guess retrieval (TIGR) database (Scott and Chédin, 1981), according to the procedure given by Sobrino et al. (1996). The outputs of applying the MODTRAN code are water vapour (figure 2), and atmospheric radiances ($R_{ati\theta\uparrow}$) and transmittances ($\tau_{i\theta}$) corresponding to the channel filter function used.

The brightness temperatures have been calculated for a large gradient of temperatures between the near surface temperature and ground surface, consisting of five surface temperatures T-5, T, T+5, T+10, and T+20, (T is the first boundary layer temperature of the atmosphere) for the daytime and three angles (0º, 22º, and 46º). Furthermore, we have used 11 different emissivities obtained from the Salisbury and D'Aria (1992) emissivity spectral responses of several types of surface (from 0.90 to 1.00). These chosen types of surfaces are representative of all the Earth's landcover. The emissivities corresponding to the AATSR channels were obtained by integration of the response functions with the appropriate emissivity spectrum.

As a result, for each type of surface, we had 9,900 different geophysical situations (60 atmospheres by 5 temperatures by 3 angles and by 11 types of surface). To simplify the simulations no aerosols have been considered. This implies that it is necessary to detect and eliminate satellite data contaminated by aerosols in order to apply the algorithms given in this document.

Once the structures of the algorithms have been determined, we selected the appropriate simulation data sets to derive the constant coefficients in the algorithms. The method used to minimize the objective function is the Levenberg-Marquardt method.

3.3.- Data Dependencies

Split-window algorithms require the following data to be available:

- Nadir 11 µm brightness temperature,
- Nadir 12 µm brightness temperature,
- Water vapour content,
- Emissivity of channel centred at 11 µm
- Emissivity of channel centred at 12 µm

4.- LSE ALGORITHM

4.1- NDVI Thresholds Method (NDVI^{THM})

Accurate algorithms for retrieving LST require the precise knowledge of the surface emissivity. LSEs are usually obtained from one TIR channel using semi-empirical approaches with vegetation indices, as for example the Normalized Difference Vegetation Index (NDVI). Of the different approaches given in the literature (Van de Griend and Owe, 1993; Sobrino and Raissouni, 2000), a modification of the last one has been used, the NDVI Thresholds Method - NDVI^{THM}.

It is a simplified method based on the estimation of emissivity, ε using atmospherically corrected data in the visible and near infrared channels (Sobrino and Raissouni, 2000), which considers three different type of pixels depending on the NDVI value: bare soil pixels (NDVI<0.2), mixed pixels ($0.2 \leq NDVI \leq 0.5$) and fully vegetation pixels (NDVI>0.5). The NDVI^{THM} have been applied for NOAA channels 4 and 5 (Sobrino et al., 2001) and for MODIS channels (Sobrino et al., 2003). The NDVI values have been calculated with the well-known equation that uses reflectivity values from the Red region (ρ_{red}) and Near Infrared (ρ_{nir}) region, according to:

$$NDVI = \frac{\rho_{red} - \rho_{nir}}{\rho_{red} + \rho_{nir}} \quad (6)$$

AVHRR channels 1 and 2, respectively centred in 0.6 μm and 0.8 μm have been used for ρ_{red} and ρ_{nir} respectively. The final expressions obtained for this method are for bare soil pixels (NDVI < 0.2),

$$\varepsilon = 0.9825 - 0.051\ \rho_{red} \quad (7a)$$
$$\Delta\varepsilon = -0.0001 - 0.041\ \rho_{red} \quad (7b)$$

for mixed pixels ($0.2 \leq NDVI \leq 0.5$),

$$\varepsilon = 0.971 + 0.018\ P_v \quad (8a)$$
$$\Delta\varepsilon = 0.006\ (1 - P_v) \quad (8b)$$

and for vegetation pixels (NDVI > 0.5),

$$\varepsilon = 0.985 \quad (9)$$

with P_v being the vegetation proportion, given by

$$P_v = \frac{NDVI - NDVI_{\min}}{\left(NDVI_{\max} - NDVI_{\min}\right)^2} \quad (10)$$

where $NDVI_{min}$=0.2 and $NDVI_{max}$=0.5. The main constraint of this method is that it can not be used to extract water emissivity values because it is not possible to apply the NDVI and P_v equations for water pixels.

5.- WATER VAPOR ALGORITHMS

5.1- Split-Window Covariance-Variance Ratio (SWCVR) technique

We use here the SWCVR (split-window covariance-variance ratio) technique to estimate total atmospheric water vapor content. This technique, based on the model of Kleespies and McMillin (1990), assumes that the state of the atmosphere is unchanged over the neighboring points where the land surface temperature and emissivities change. Thus, considering adjacent pixels is possible to obtain

$$W = \frac{(G_5 - G_4)}{(A_5 - A_4)} * W_{GAS} - \frac{1}{(A_5 - A_4)} * \cos\theta \ln R_{54} \tag{11}$$

where θ is the angle of observation, A_k and G_k (k=4,5) are the band-average absorption coefficients in Channels 4 and 5 of the AVHRR, for water vapor and other gases, respectively, W and W_{GAS} are, respectively, the total effective contents of water vapor and other gases, and R_{54}, that represents the ratio between the AVHRR Channels 5 and 4 transmissivities and emissivities (i.e., $R_{54} \approx \varepsilon_5 \tau_5 / \varepsilon_4 \tau_4$) can be mathematically expressed as (Sobrino et al., 1994)

$$R_{54} = \frac{\sum_{K=1}^{N} (T_{4k} - T_{40})(T_{5k} - T_{50})}{\sum_{K=1}^{N} (T_{4k} - T_{40})^2} \tag{12}$$

where the numerator and denominator of (12) represent, respectively, the covariance and the variance of brightness temperatures directly measured by the satellite in AVHRR Channels 4 (T_4) and 5 (T_5) with T_{40} and T_{50} being the mean temperature of the pixels considered in each channel.

6.- VALIDATION PLAN

To validate the proposed algorithm we used a set of 300 LSTs measured in situ in two regions of Australia (Prata, 1993). We used this validation dataset because it is the best available in terms of accuracy and size. With these data, the estimated error in land surface temperature is of the order of 1.3K. The error in water vapor is of the order of 0.5 g.cm^2, leading to errors in LST lower than 0.6 K.

7.- COMPUTATIONAL CONSTRAINTS, LIMITATIONS, AND ASSUMPTIONS

The split-window algorithm developed for AVHRR data can be applied in general conditions and provides satisfactory results whenever the input data is accurate.

The quality of the thermal parameters is critically dependent upon the quality of the brightness temperatures (e .g. calibration of the images) and it is necessary to carry out a cloud mask over the whole image.

The major source of error in the algorithms is the emissivity uncertainty.

8.- CLOUD TESTS

Residual clouds are present in the data in spite of the compositing procedure applied to the data (Maximum Value Compositing, Holben, 1986), especially in areas with persistent cloud cover, such as tropical areas. Therefore, a cloud screening is needed in order to observe land surface temperatures corresponding to actual surface values.

Saunders and Kriebel (1988) developed a series of 5 tests for cloud detection from AVHRR data. Those 5 tests require nighttime and daytime images of AVHRR channels 1, 2, 3, 4 and 5. As neither nighttime nor channel 3 data are publicly available, only 3 tests have been applied to LST data out of the 5 tests described by Saunders and Kriebel (1988).

8.1- Dynamic reflectance threshold test

In a general manner, clouds have a higher reflectance than land or sea surface, as shown in figure 1. This means that over land and sea, a cloud-free reflectance peak can be identified in the histogram of the image, allowing a threshold to be set at a slightly higher reflectance. Thus, all pixels with reflectances above this threshold are considered as cloud contaminated. Identifying a cloud-free reflectance peak and then setting a threshold value removes uncertainties due to variation in calibration and changes in surface reflectance with solar zenith/azimuth angles. Over land, channel 1 reflectances are used since the reflectance in channel 1 is much less than in channel 2, which increases the contrast between land and cloud (Saunders, 1986).

8.2- Reflectance ratio test

This test makes use of the ratio of near-infrared bidirectional reflectances (AVHRR channel 2) to visible bi-directional reflectances (AVHRR channel 1). This ratio test can be simplified to the following expression (Saunders & Kriebel, 1988):

$$Q = \frac{Ch2}{Ch1}$$

This ratio is close to unity over clouds (Figure 1), while over water this ratio is close to 0.5. Over land, Q is greater than unity for all cases (vegetation, desert) except for snow and ice, even if there is often no well-defined peak due to the large variability of this ratio over land. Thus, a default threshold of 1.6 is set, while all pixels with a lower value of Q are assumed to be cloud-contaminated (Saunders and Kriebel, 1988).

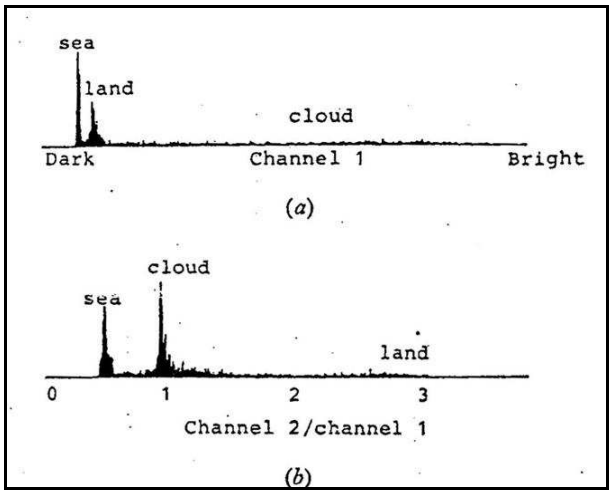

Figure 1.- Histograms of NOAA-9 AVHRR data for 15 April 1985 over the United Kingdom, containing clouds, cloud-free land and ocean. (a) Channel 1 reflectance; (b) channel 2 / channel 1 reflectance ratio histogram (adapted from Saunders and Kriebel, 1988, figure 1).

8.3- Radiometric temperature difference test

This third test examines the difference between the 11 μm (AVHRR channel 4) and 12 μm (AVHRR channel 5) brightness temperatures. This difference tends to increase in presence of clouds, due to differences in transmittance between those wavelengths. Thus, threshold values have been estimated for this difference, above which the pixels are considered as cloud-contaminated. Table 1 shows those threshold values for mid-latitudes (Saunders & Kriebel, 1988).

Table 1.- Temperature thresholds Tdiff for the Ch4 – Ch5 cloud detection test at mid-latitudes (adapted from Saunders & Kriebel, 1988, table 1).

T_{11} (in K)	260	270	280	290	300	310
T_{diff} (in K)	0.55	0.58	1.30	3.06	5.77	9.41

8.4- Additional cloud test

Cloud tests 1 and 2 tend to overestimate cloud contamination, therefore these two test were conditioned to an additional one, which only considers as possibly cloud-contaminated the pixels for which LST value is below 280 K. This allows the distinction between high reflectance areas (deserts) and clouds.

ACKNOWLEDGMENTS

We wish to thank the European Union EAGLE project (SST3-CT-2003-502057), the Ministerio de Ciencia y Tecnología (DATASAT, project ESP2005-07724-C05-04) and the European Union WATCH integrated project (Contract Number 036946) for their financial support, and also to the people from the Global Change Unit and the Solar Radiation Unit, University of Valencia for their help in the field campaign. Source for the PAL dataset was the Goddard Earth Sciences Distributed Active Archive Center in 2004 (data unavailable in 2008).

REFERENCES

Abreu, L. W., and Anderson, G. P., (Eds.), (1996). The MODTRAN 2/3 report and LOWTRAN 7 model, *Modtran Rep., Contract F19628-91-C-0132*, Phillips Lab., Hanscom Air Force Base, Massachussets.

Becker, F. and Li, Z.-L. (1990). Temperature-independent spectral indices in thermal infrared bands, *Remote Sens. Environ. 32*, 17-33.

Grant, W. B. (1990). Water vapor absorption coefficients in the 8 – 13 mm spectral region: a critical review. *Applied optics*, 29, 451-462.

Holben, B. N. (1986). Characteristics of maximum-value composite image from temporal AVHRR data. *International Journal of Remote Sensing*, 7: 1417-1434.

Klesspies T. J. and McMillin, L. M. (1990). Retrieval of precipitable water from observations in the split-window over varying surface temperature. *J. Appl. Meteorol.*, vol. 29, pp. 851–862.

McClain, E. P., W. G. Pichel and C. C. Walton, (1985). Comparative Performance of AVHRR-based Multichannel Sea Surface Temperatures, *Journal of Geophysical Research*, *90*, 11587-11601, 1985.

Prata, A. J. (1993). Land surface temperatures derived from the AVHRR and ATSR, 1 Theory, *J. Geophys. Res.,* 89D9, 16689-16702

Price, J.C. (1984). Land surface temperature measurements from the split window channels of the NOAA-7 AVHRR. *J. Geophy. Res. 79*, 5039-5044

Salisbury, J. W., and D. M. D'Aria, Emissivity of terrestrial materials in the 8-14 μm atmospheric window, *Remote Sensing of Environment, 42,* 83-106, 1992.

Saunders, R. W. (1986). An automated scheme for the removal of cloud contamination from AVHRR radiances over western Europe. *International Journal of Remote Sensing*, 7, 867.

Saunders, R. W. and Kriebel, K. T. (1988). An improved method for detecting clear sky and cloudy radiances from AVHRR data. *International Journal of Remote Sensing*, 1988, Vol. 9, No. 1, 123-150.

Scott, N. A., and A. Chédin, A fast line by line method for atmospheric absorption computations: The Automatized Atmospheric Absorption Atlas, *Journal of Applied Meteorology, 20*, 802-812, 1981.

Sobrino, J.A., Li, Z.-L., Stoll, M.P., and Becker, F. (1994). Improvements in the split-window technique for the land surface temperature determination. *IEEE Trans. Geosc. and Remote Sens.,* Vol. 32, No. 2, 243-253

Sobrino, J.A., Li, Z.-L., Stoll, M.P., and Becker, F. (1996). Multi-channel and multi-angle algorithms for estimating sea and land surface temperature with ATSR data. *International Journal of Remote Sensing, 17*, 2089-2114.

Sobrino, J.A. and Raissouni, N. (2000). Toward remote sensing methods for land cover dynamic monitoring: application to Morocco. *International Journal of Remote Sensing.* 21 (2) 353-366

Sobrino, J. A., Raissouni, N. and Li, Z.-L., 2001. A comparative study of land surface emissivity retrieval from NOAA data, *Remote Sensing of Environment*, 75:256-266.

Sobrino, J. A., J. El Kharraz, and Z.-L. Li, 2003. Surface temperature and water vapour retrieval from MODIS data, International Journal of Remote Sensing, 24(24), 5161-5182.

Van de Griend, A. A., and Owe, M., 1993. On the relationship between thermal emissivity and the normalized difference vegetation index for natural surfaces, International Journal of Remote Sensing, 14(6):1119-1131.